# Effect of Vegetable-Based Polyols in Unimodal Glass-Transition Polyurethane Slabstock Viscoelastic Foams and Some Guidance for the Control of Their Structure–Property Behavior. II

**Benjamin R. Vaughan,[1] Garth L. Wilkes,[1] Dimitrios V. Dounis,[2] Cam McLaughlin[2]**

[1]*Department of Chemical Engineering, Virginia Polytechnic Institute and State University, Blacksburg, Virginia 24061*
[2]*Hickory Springs Manufacturing Company, P.O. Box 2948, Hickory, North Carolina 28603*

Received 1 August 2009; accepted 25 May 2010
DOI 10.1002/app.32864
Published online 9 September 2010 in Wiley Online Library (wileyonlinelibrary.com).

**ABSTRACT:** Building on the dynamic mechanical analysis (DMA) characterization of the viscoelastic (VE) foam materials discussed in part I of this two-part sequential series of articles, in this second part, we provide further information on the general physical properties of many of the same soy polyol and castor-oil VE foams. In particular, the tensile, tear, elongation, indentation force deflection, support factor, compression set, hysteresis and ball-rebound (resilience), and density properties are addressed in this article. The air flow and force buildup after compression deformation are also considered. Particular attention is also given to noting the degree of correlation of ball-rebound behavior to that of the DMA damping data provided in part I. We concluded that when all of the properties of these vegetable-based VE foams were taken as a whole, they had acceptable structure–property behaviors for VE applications, although certainly, the formulations could undoubtedly be further fine-tuned for additional optimization. © 2010 Wiley Periodicals, Inc. J Appl Polym Sci 119: 2698–2713, 2011

**Key words:** foam extrusion; polyurethanes; structure–property relations

## INTRODUCTION

In part I of this two-part series, we principally addressed the dynamic mechanical analysis (DMA) behavior, cellular morphology, and some information regarding the rise and reaction temperature profiles during the foaming of several viscoelastic (VE) polyurethane foams (PUFs) synthesized with the incorporation of either soy-oil-based polyols or castor oil (a polyol of natural origin). More specifically, the use of DMA and, specifically, tan δ was focused on as an index of the damping behavior of these foams, a property that is extremely important for VE PUFs. It is also surprising that there are other mechanical properties that are of considerable importance to the utility of VE PUFs, and these include the air flow through the foam, indentation force deflection (IFD), support factor (SF), compression set, tear, tensile properties, elongation, hysteresis, and ball rebound; the last variable is also a standard measure of the resilience behavior of foams.[1] In contrast, however, to the damping expressed by tan δ, the ball rebound is not necessarily a linear VE parameter; when a ball is dropped onto a foam surface, the ball may well exceed the local linear VE deformation limit, and also, the rate or loading varies (slows to zero) after the ball impinges the foam surface; hence, it is not a single-loading-rate experiment as is tan δ for a fixed oscillatory frequency. With the exception of the peak tan δ value at the glass-transition temperature ($T_g$), other values from the same dispersion region are typically double valued because of the near symmetry about the peak value at a given frequency. However, the modulus is quite different for any pair of equal tan δ values because, on the lower temperature side, the modulus is higher than on the upper temperature side of the peak. This differentiation is more extreme as one moves further from either side of the dispersion peak, and the variation in the modulus with temperature will also typically be dependent on the breadth of the dispersion. Certainly, the relative stiffness is important in a ball-rebound experiment because a stiffer foam (low-temperature side) will not lead to as much deformation as when that same loading occurs on the higher temperature side of the $T_g$ dispersion. In short, although one would hope that there is a good correlation of the tan δ behavior with that of ball rebound, the question remains as to whether such a correlation exists between these two

*Correspondence to:* G. L. Wilkes (gwilkes@vt.edu).
Contract grant sponsor: United Soybean Board.

quite different types of measurements across the full $T_g$ tan δ dispersion. We focus on this issue later in this article.

In addition to the several properties specified previously, many of which are addressed within this part of our two-part series, we also consider some limited measurements of the effect of the relative humidity (RH) at selected temperatures on some specific properties. Clearly, such information is of value because PUFs are distinctly susceptible to moisture pickup because of their inherent polar characteristics, as promoted by the occurrence of urethane and urea linkages and others polar groups, such as ester and/or ether groups, depending on the specific polyol chemistry used.

Because pertinent reference material regarding the nature of VE PUFs is provided in part I, which precedes this report in this same journal issue, we do not restate this same material here. However, we do point out that in addition to the damping character of a VE PUF, the other physical properties stated previously are obviously of significance to the structure–property behavior and the applicability of such foams, and thus, some additional remarks are in order concerning these parameters.

The air flow rate through the foam is distinctly dependent on the cell openness promoted by the minimization of closed cell windows at the end of the foam synthesis. The cell size and its distribution may also influence air flow. However, air flow can also be greatly enhanced, as is often done industrially, by mechanical crushing of the foam after synthesis, which helps to promote the breaking of some of the existing cell windows. This process is common for molded high-resilience foams, in particular, but also for certain VE PUFs that are made by the slabstock methodology. In this article, we only focus on the air flow values of the crushed foams unless otherwise stated. The generalized procedure of crushing is given in part I, but we review it briefly in the Experimental section of this article. Also, in contrast to part I of this series, in which we treated the soy-based VE PUFs separately from those based on castor oil, here, we combine the data from both vegetable-oil-based systems because it more easily allows direct comparisons in many cases. We also, with some degree of hesitation, include many of these same physical properties for the same example commercial slabstock VE foam used in part I for purposes of comparison. However, our hesitation to enter these data is that the direct comparison of these specific parameters with those of the soy-based or castor-oil foams is somewhat limited by the large difference in density between the commercial VE PUF and those that we synthesized. As stated in part I of this series, the density of the example VE foam was 5.33 pounds per cubic foot (pcf), whereas the general range of density of our vegetable-based foams was 2.5–3.0 pcf. This density difference could have influenced many of the mechanical properties that we discuss, so keep this issue in mind when comparisons are made later in this article.

The foam materials we discuss were prepared by a box foam process, which mimics a slabstock process, including the development of anisotropy of the cellular texture during foam rise because the shape of the forming cells often become partially elongated along the rise or blow direction of the foam. This anisotropy could have distinctly influenced the directionality of many of the mechanical properties. Cell nucleation in a box process is also not necessarily equivalent to that generated in an industrial slabstock continuous line, but the trends shown by box foams typically mimic those from a commercial process if the same formulations are used. For example, the modulus will be higher in compression when the loading direction is along the rise axis.[2] Typically, slabstock PUFs used in cushioning applications are cut so that the loading direction is parallel to the rise direction of the foam. Many other mechanical properties can likewise display directionality dependence as well. Also, the compression–load behavior, its rate dependence, and any other pertinent variable (e.g., RH or temperature) will clearly influence the profile of the cushioning behavior of the foam; this is important with respect to what is sensed as comfort.[1,3–11] Certainly, it is also not surprising that because of the multiple loadings or deformations of a foam cushion in use, its tear, elongation, and related mechanical characteristics are relevant to the perceived quality and durability of a given foam. As might be expected, the cyclic fatigue of PUFs is also of importance, but this specific topic is not addressed in our report. As a result of the need for characterizing such mechanical parameters, as might be expected, many ASTM protocols have been put into place such that the various producers of foams can undertake such applied tests that allow interlaboratory comparisons. Furthermore, it is recognized that the performance of such tests on laboratory-scale-produced foams, such as the box foams discussed in this report, may require some modifications of the test protocols, but the test results are still of great value in the characterization and comparison of different foam chemistries or process modifications for producing the foams. Good references that provide more details of the pertinent ASTM tests can be found in several standard sources.[1,3]

With this discussion as a backdrop and in conjunction with the introductory material given in part I of this report, we now address the experimental procedures used and provide a quick review of the preparation of the vegetable-oil-containing VE PUFs that were discussed in part I.

## EXPERIMENTAL

### Unit conversion

Some of the units reported in this report and in part I of this series are foam industry standard units. Thus, for convenience, we provided a table in part I with conversions from English units to meter, kilogram, second (MKS) metric units.

### Materials

The petroleum-based polyol used in this study, Softcel U-1000, was donated by Bayer MaterialScience (Pittsburgh, PA). Soy-based polyol Agrol 3.0 was donated by Biobased Technologies (BBT, Fayetteville, AR). For simplicity, from this point on, we refer to this polyol by its supplier and polyol hydroxyl number (BBT-99). United States Pharmacopoeia grade castor oil (OH# 166) was purchased from Fisher Scientific (Waltham, MA). A leading VE foam producer kindly supplied a typical 5.33 (pcf) VE slabstock foam sample for comparison. The catalysts, surfactants, additives, and toluene diisocyanate (TDI) used in the foam formulation were graciously provided by Hickory Springs MFG (Hickory Springs, NC). The catalysts used in the formulation were DABCO T-12 and DABCO 33LV from Air Products and ZF24 from Huntsman Corp. (Allentown, PA). The additives used in the formulation were DP-1022 from Momentive Performance Materials (Albany, NY), Firemaster 550 from Chemtura (Middlebury, CT), and glycerol triacetate (GTA) from Fisher Scientific. The surfactant used in the formulation was L-618 from Momentive Performance Materials. The 80/20 TDI used in this study was a product of Bayer.

### VE foam synthesis

The PUFs (target density = 2.7 pcf) were synthesized with the formulation listed in Table I. Approximately 400 g of reagents was mixed with a size #2 ITT CONN blade in a 92-oz polypropylene cup at 2000 rpm and poured into a 10 × 10 × 4 in.$^3$ cake box to rise and cure. The rise height and temperature were monitored and recorded for 5 min with an ultrasonic cone and thermocouple (Keyence, Osaka, Japan), the latter of which was placed into the reacting system but away from any edge of the box. After 5 min, the foam was placed in an oven at 240°F for 25 min of postcuring in an attempt to simulate the curing conditions in a large bun. The samples were allowed to sit for 3 days before they were cut from the boxes and crushed parallel to the rise direction of the foam with mechanical rollers and conditioned according to ASTM D 3574 for physical testing.

**TABLE I**
**VE Foam Formulation Used in This Study**

| Reagent | Formula (pph) |
|---|---|
| Polyol | 98.80 |
| DP-1022 | 1.20 |
| Firemaster 550 | 1.00 |
| Water | 1.90 |
| Silicone surfactant (L-618) | 0.50 |
| TD-33 (33LV) | 0.21 |
| ZF24 | 0.21 |
| Tin catalyst (T-12) | 0.03 |
| Tin catalyst (T-9) | 0.00 |
| TDI 80/20 index | 96 |

pph = parts per hundred; index = isocyanate/hydroxyl × 100.

### Characterization methods

#### Physical properties

Unless otherwise stated, ASTM and modified ASTM standard methods were used for physical property measurements. The samples were conditioned at 50 ± 5% RH and 23 ± 3°C. Also, unless otherwise specified, all measurements were made parallel to the rise direction on samples cut to 8 × 8 × 3 in.$^3$ Before the samples were mechanically crushed, the foam density was measured according to ASTM D 3574-A, and air flow after crushing was measured with a modified BASF air flow tester (Ludwigshafen, Germany) according to ASTM D 3574-G. All other tests were performed on samples crushed with a mechanical roller–crusher in two directions with a gap proportional to 10% of the original height of the foams. IFD measurements (25, 65, and 25% return) were made on a Hickory Springs MFG house-built IFD tester according to ASTM D 3574-$B_1$. The conventional SF parameter was then calculated as the ratio of the 65% IFD value to the 25% IFD value. Hysteresis was also calculated with the IFD values according to eq. (1)[1]:

$$\text{Hysteresis } (\%) = \frac{25\% \text{ Return IFD}}{25\% \text{ Original IFD}} \times 100\,\text{s} \quad (1)$$

Ball rebound or resilience was measured according to ASTM D 3574-H with a Time Tech, Inc., TT502 ball-rebound tester (Chicago, IL). Tensile, tear, and elongation testing was performed on samples according to ASTM D 3574-E,F with a GCA/Precision Scientific Scott-CRE/500 tensile and compression tester. Measurements of 50% compression set were made according to ASTM D 3574-D. Samples tested for resilience or ball rebound as a function of the temperature/humidity were cut into 6 × 6 × 1 in.$^3$ slabs. Recovery was measured on all samples with a FACT Series I automated compression tester (Intelimetrics,

**TABLE II**
**Physical Properties of the Commercial VE Slabstock Foam**

| | | | |
|---|---|---|---|
| Density (pcf) | 5.3 | 25% IFD (lb/50 in.$^2$) | 13.0 |
| Air flow (SCFM) | 1.5 | 65% IFD (lb/50 in.$^2$) | 25.4 |
| Tensile (psi) | 8.5 | 25% return (lb/50 in.$^2$) | 12.1 |
| Tear (pli) | 1.8 | Hysteresis | 93.3 |
| Elongation (%) | 247 | SF | 1.95 |
| Ball rebound (%) | 1 | 50% compression set (%) | 0.76 |

$T_g$ = 17°C (tan δ peak at 1 Hz).

Inc., Chester, SC) at 21°C and 46% RH according to ASTM D 3574-M, except for the smaller sample size. Select samples were conditioned in a Cincinnati Sub-Zero environmental chamber (Cincinnati, OH) at specific humidities and temperatures. The temperature and humidity conditions chosen for the ball-rebound measurements were as follows: 0°C and 65% RH, 55°C and 50% RH, 75°C and 50% RH, 21°C and 17% RH, 21°C and 46% RH, and 21°C and 80% RH.

After conditioning, resilience was measured with an automated Laser Array ball-rebound tester constructed in accordance with Bayer specifications.

As stated earlier, one sample commercial VE slabstock foam was also used in some cases for comparison with the laboratory-synthesized foams. The properties of this foam are reported in Table II. We used the same specimen sizes of this foam for the tests as were used for the vegetable-oil-based foams. Recall that the density of the commercial VE foam was higher than that of the synthesized foams. Therefore, as stated earlier, care must be taken to consider this difference in density when comparisons are made with the other PUFs.

Scanning electron micrographs of several of the foam cellular textures were obtained with a LEO (Zeiss) 1550 field emission scanning electron microscope with an SE2 detector set at 10 kV with a working distance (WD) of approximately 24 mm.

We measured the sol fraction by submerging samples (34 × 34 × 5.5 mm$^3$) in an excess of dimethylacetamide for 24 h at 50°C with gentle oscillation every 4 h for 5 min to redistribute any concentration gradients. The samples were then dried in a convection oven at 60°C overnight and further dried under full vacuum (30 mmHg) at 65°C for 24 h before the final weight was recorded. The results are reported as percentage sol fraction.

## RESULTS AND DICUSSION

### Sol contents and $T_g$ behavior

Because both the sol content and $T_g$ (from the tan δ peak at 1 Hz) were of significance in understanding some of the trends of the mechanical behavior of the foams, we provide that information first in Figure 1(a,b). Of relevance in Figure 1(a) is that, as expected, the sol content increased as the isocyanate index decreased for both the castor-oil foam and those containing soy polyols. This information is useful in accounting for some of the mechanical properties discussed later. Also, the $T_g$ data in Figure 1(b) shows $T_g$ as a function of the percentage soy polyol content, where the specific polyol had a fixed hydroxyl number of 99 for all of the samples in the U-1000–soy series. As the content of this polyol was increased from 0 to 50%, the $T_g$ value increased from 17 to about 22°C; this clearly showed that this particular hydroxyl number polyol slowly shifted $T_g$ upward with increasing soy composition. As a VE foam was used in the general range of its $T_g$ and it was this range in which there were

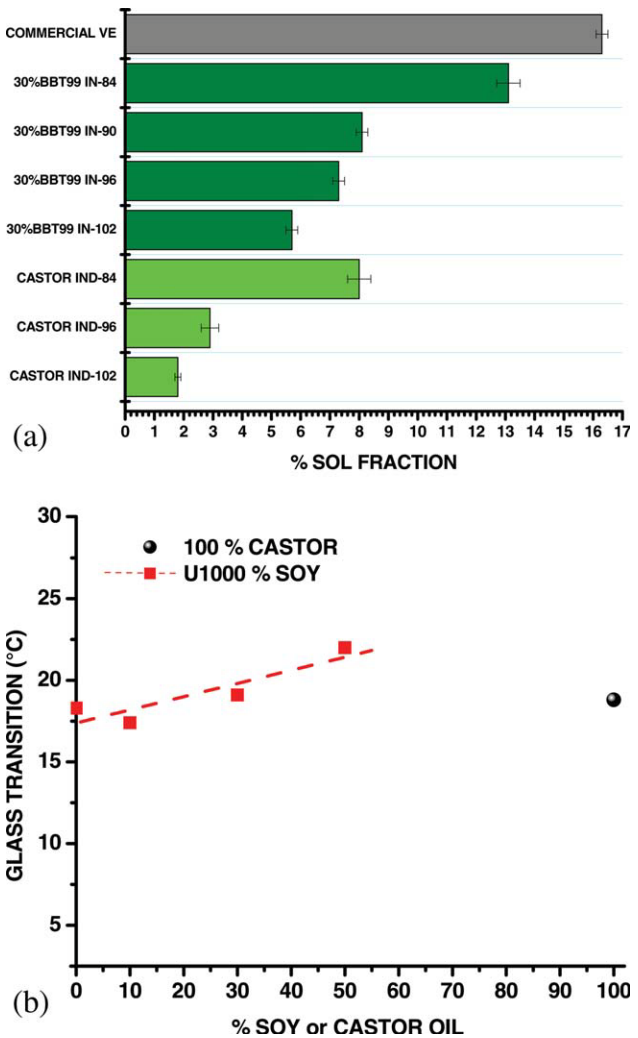


**Figure 1** (a) Sol fraction for the U-1000–30% soy and 100% castor-oil foams and the commercial VE foam as a function of the isocyanate index and (b) $T_g$ for the soy and castor-oil VE foams (index = 96) as a function of vegetable-oil content. IN and IND = index. [Color figure can be viewed in the online issue, which is available at wileyonlinelibrary.com.]

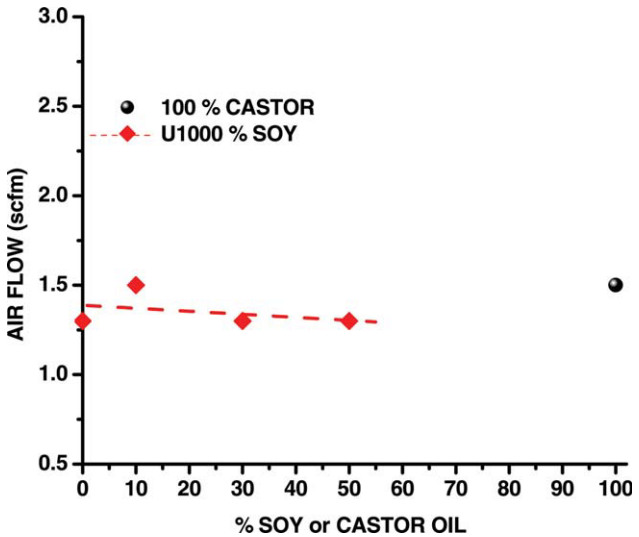


**Figure 2** Air flow for the soy and castor-oil VE foams (index = 96) as a function of the vegetable-oil content. [Color figure can be viewed in the online issue, which is available at wileyonlinelibrary.com.]

major changes in the properties with temperature, what appears in Figure 1(b) as a relatively small thermal range still had significant consequences on the other associated mechanical properties, as is soon discussed. Also, as shown in Figure 1(b), the 100% castor-oil foam possessed a $T_g$ of 18°C (tan δ peak at 1 Hz) and was, thus, very similar in its $T_g$ behavior to that of the U-1000 polyol foam, which contained no vegetable-oil polyol. (We point out that for comparison, the sample commercial VE foam discussed earlier in part I possessed a $T_g$ of 17°C, which was very close to that of the castor-oil foam.) The corresponding air flow data for these same respective foams are given in Figure 2, which indicates that addition of soy polyol up to a 50% content with U-1000 had little effect on the air flow, for the values hardly changed from about 1.4 standard cubic feet per meter (SCFM). Furthermore, the corresponding value for the 100% castor-oil foam was also only slightly higher and was about 1.5 SCFM. Thus, the data in total suggest that there seemed to be little effect on the air flow with these specific vegetable-based polyol foams relative to the foams made with only the petroleum-based U-1000 polyol. Also, the air flow value for the sample commercial foam was also 1.5 SCFM; for at least for this important variable, there was alignment with both of the vegetable-oil-based foams.

### Tensile strength, tear, elongation, compression set, and force recovery behavior

Turning first to the ultimate properties of tensile strength, tear strength, and elongation to break, we

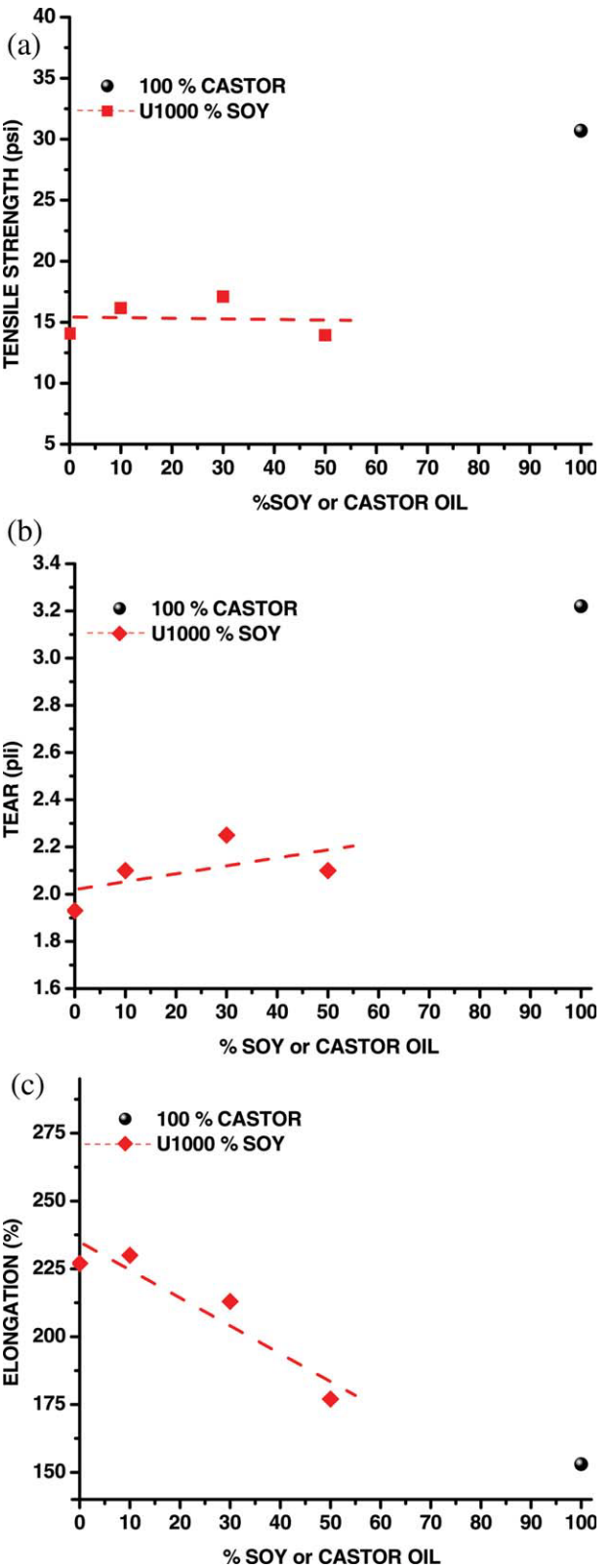


**Figure 3** (a) Tensile strength, (b) tear strength, and (c) elongation for the soy and castor-oil VE foams (index = 96) as a function of the vegetable-oil content. [Color figure can be viewed in the online issue, which is available at wileyonlinelibrary.com.]

show the results for these three parameters in Figures 3(a–c), respectively. Addressing first the series of foams containing a portion of soy polyol, we note that with the addition of the soy polyol, the foam properties did not greatly change relative to the foam with no soy polyol. In fact, there was minimal dependence on the soy content for the tensile and tear behavior in this range of composition. Furthermore, the elongation, although it decreased systematically with soy content, only dropped from about 230 to 175% over the full range, which was not a major change for this ultimate property. Also, we observed a single point value for the 100% castor-oil-based foam. We observed that the 100% castor-oil foam had a distinctly higher tensile and tear strength than the soy-based materials just discussed. Interestingly, it was also lower in elongation than the soy-containing foams; however, it was nearly in line with the extrapolated elongation value for a 100% soy-containing foam, shown in Figure 3(c). This may have been due to the fact that vegetable-based polyols, other factors being equal, all possess the presence of the short dangling chain beyond where the functional hydroxyl group resides; these may lead to poorer network development relative to most petroleum-based systems of equal index, and thus, a lower elongation might be expected. This, however, is only a hypothesis at this stage because further work would be needed to test this conjecture. Also, in view of the castor-oil-based foam possessing an intermediate $T_g$ relative to all others in this group, any differences in the tear, elongation, or tensile behavior could not be argued on the basis of such differences. Although the results are not shown here, the 50% compression set for these same foams was less than 4% and hardly changed for all the of the previously discussed materials; this suggests that the substitution of these specific vegetable-based polyols did not alter this important parameter in any major way relative to the foam based solely on the petroleum polyol, U-1000. (The compression set for the sample commercial VE foam was also lower than 4% as well.)

Finally, if one recalls Table I, which displays the values for the tensile, tear, and elongation behaviors for this same foam, the values were 8.46 psi, 1.79 pli, and 247%, respectively. The fact that the tensile and tear values were on the lower sides of the values for the vegetable-oil-based foams suggests that the commercial VE foam was either softer or weaker at the test temperature used because its density was about a factor of two greater than either of the two types of vegetable-oil foams. As shown by the DMA behavior of the commercial VE foam discussed in part I, this material had a particularly narrow tan δ transition dispersion, such that at a test temperature of 23°C, it was already quite low in modulus; this may help explain why the tensile and tear values were lower than those of the vegetable-oil foams, although the tensile or tear force was acting on nearly double the amount of material per unit area during the test relative to the vegetable-oil-based foams. Other potential differences in the network structure could have also been relevant, for the sol content of the commercial VE foam was quite high; this indicated many unconnected species in its structure as well. With regard to the variable of elongation, the value of the commercial VE material (247%) was within the same range as the values of the U-1000 foams.

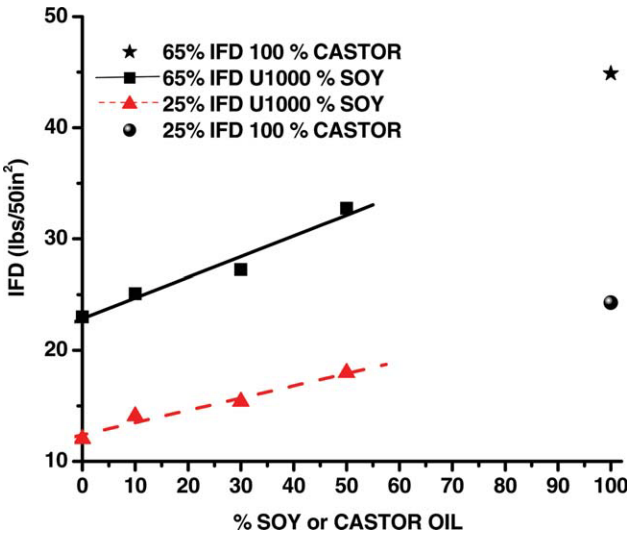


**Figure 4** 25% IFD and 65% IFD for the soy and castor-oil VE (index = 96) foams as a function of the vegetable-oil content. [Color figure can be viewed in the online issue, which is available at wileyonlinelibrary.com.]

Figure 4 shows both the 25 and 65% IFD values for the foams being discussed, and the plots indicate that each of these parameters increased systematically with soy content relative to the U-1000 foam without soy content. The values for the commercial VE foam were also nearly equivalent to that of the U-1000 foam as well (recall Table I). Because the density of the VE foam was much higher than the U-1000 system, it was clear that the network of the commercial VE foam must have been of lower modulus or stiffness (per actual unit mass) because nearly twice the amount of material was compressed during its IFD test relative to the U-1000 foam. With regard to the 100% castor-oil foam, it had a higher IFD value than the designated soy-containing foams, but we believe this may have been due to the fact that this system had the lowest sol fraction of all and, thus, a tighter network because of its natural hydroxylation. Recall from Figure 1(a) that the sol fraction was lowest for this material. Furthermore, in the respective DMA plots from part I for both the soy foams and castor-oil foams for the same index

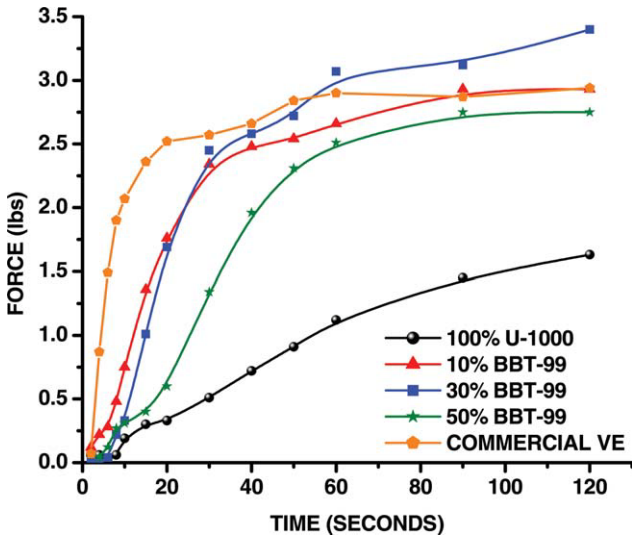


**Figure 5** Force recovery for a commercial VE foam compared with synthesized VE foams as a function of the soy content. [Color figure can be viewed in the online issue, which is available at wileyonlinelibrary.com.]

value of 96, we found that at the same temperature as was used for the IFD tests, it was the castor-oil foam that possessed the higher modulus; this would principally account for why this foam had the higher IFD values for both the 25 and 65% deflections. Interestingly, when the SF was calculated (the ratio of 65% IFD to 25% IFD), we found that all of the foams only randomly varied in the range of about 1.75–1.95, which was not a major change. (The commercial VE foam also possessed an SF value of 1.95.)

In addressing the recovery kinetics following the compression of the foam to 25% of the height of its original thickness measured at 1 lb of force at ambient conditions, in Figure 5, we show the force recovery over the first 120 s for the commercial VE PUF and the behavior of the soy-based foams discussed previously and, finally, that of the pure U-1000 foam (no soy). The behavior for the castor-oil-based foam is not shown here; it is provided later when the variable of foam index is addressed. From this figure, we noted that the commercial VE foam displayed a faster force rise with time compared to the U-1000 foam with no soy. One distinct reason this occurred, of course, was, again, that the commercial foam was denser than that of all the other foams. However, when soy polyol was incorporated into U-1000, the force rise with time was closer for the same time frame to that of the commercial VE foam.

### Effect of the foam index and plasticizer content on properties and structure

We now turn our attention to the influence of foam index (isocyanate/hydroxyl ratio × 100) and plasticizer content on some of the same mechanical properties discussed previously. As we show, the addition of plasticizer also had a very pronounced effect on the cell morphology in the specific case of the castor-oil foam. We first address the variable of index. In the case of the single soy-containing foam that we used, we maintained the soy content at its highest level (30%) and the hydroxyl number constant at 99. For the case of the castor-oil foam, the polyol content was again 100% castor oil. The isocyanate index level was then decreased systematically from 102 to 84, which was the same range used in the DMA study discussed in part I of this two-part series. Figure 6(a) shows how $T_g$ for both types of foams (soy-containing and 100% castor) behaved with index. Each one systematically decreased with decreasing index with the same level of dependence

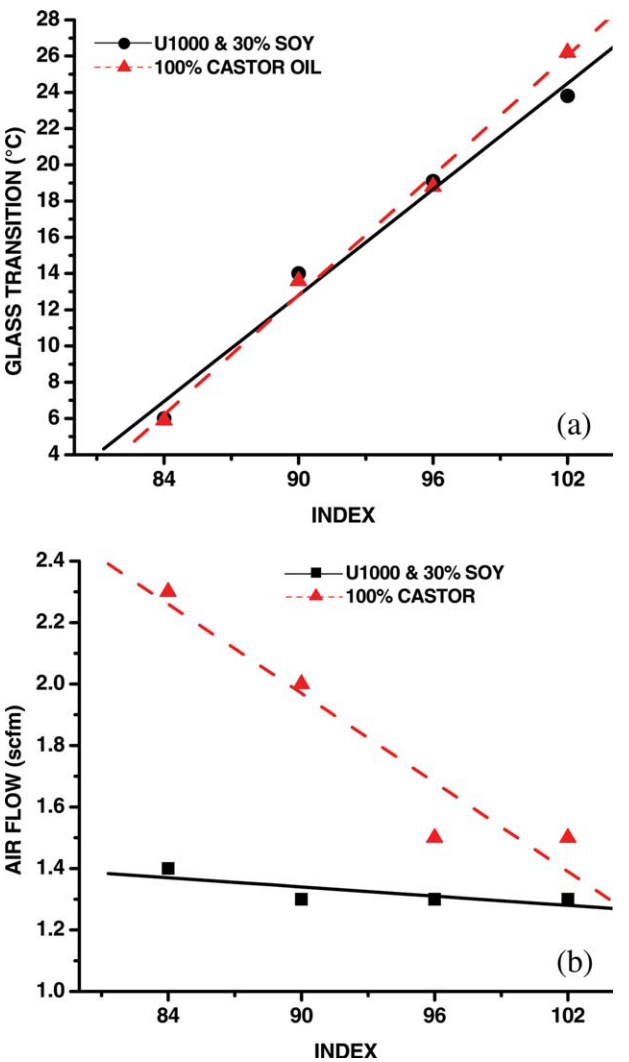


**Figure 6** (a) $T_g$ and (b) air flow for the U-1000–30% soy and 100% castor-oil VE foams as a function of the isocyanate index. [Color figure can be viewed in the online issue, which is available at wileyonlinelibrary.com.]

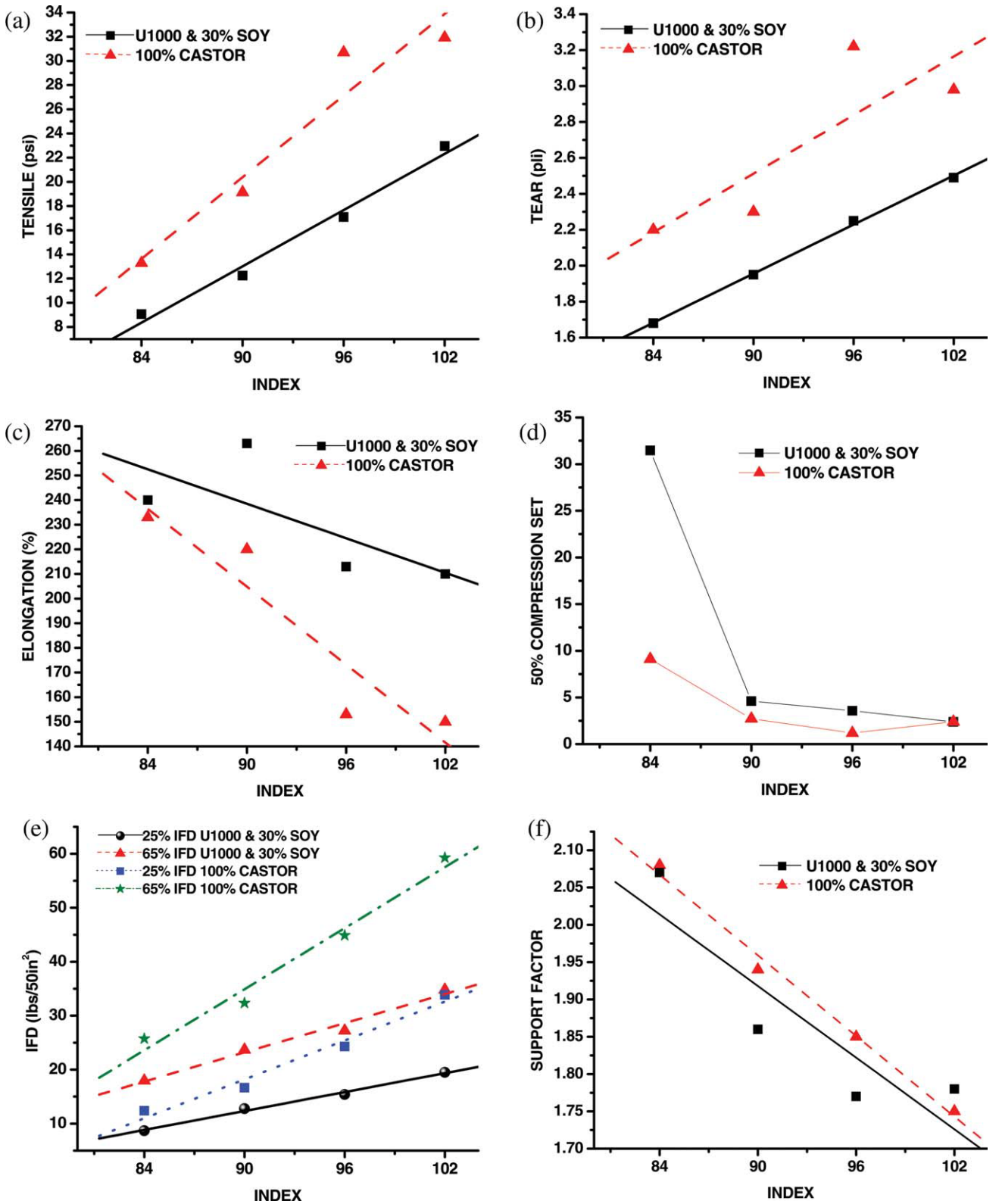


**Figure 7** (a) Tensile strength, (b) tear strength, (c) elongation, (d) 50% compression set, (e) 65% IFD and 25% IFD, and (f) SF of the U-1000–30% soy and 100% castor-oil foams as a function of the isocyanate index. [Color figure can be viewed in the online issue, which is available at wileyonlinelibrary.com.]

on this parameter. For every 6% drop in index, there was a corresponding 6.6°C decrease in $T_g$ for the castor foams and a 5.6°C decrease in $T_g$ for the U-1000–soy-containing foams. Regarding air flow, Figure 6(b) shows that the air flow for the soy-containing foams had little dependence on the index

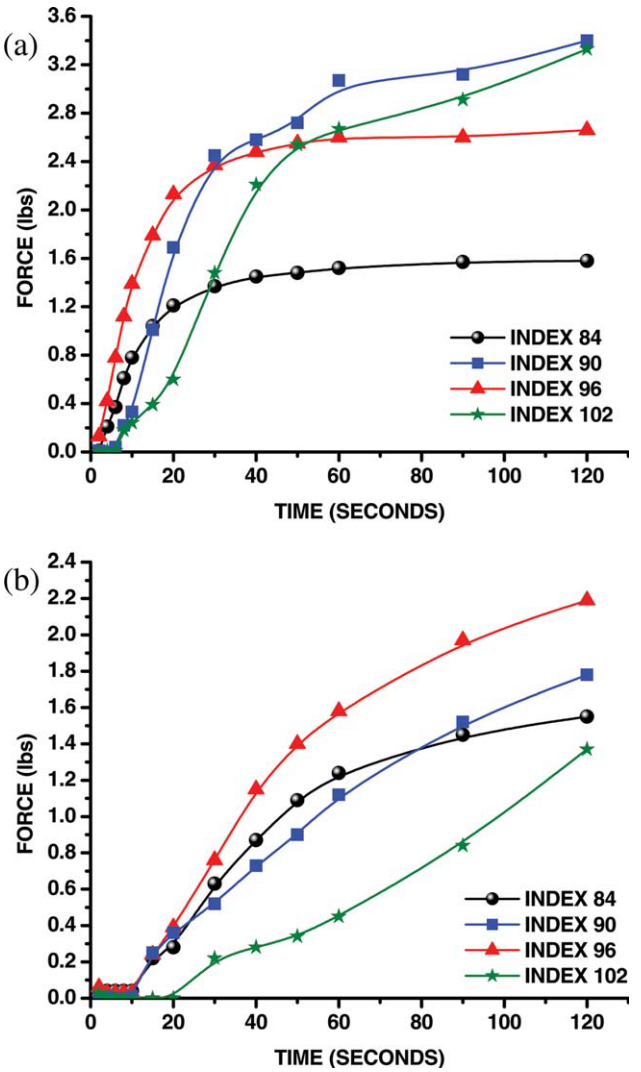


**Figure 8** Force recovery of the (a) U-1000–30% soy foams and (b) 100% castor-oil foams as a function of the isocyanate index. [Color figure can be viewed in the online issue, which is available at wileyonlinelibrary.com.]

over this range, whereas there was a very distinct systematic decrease in the air flow with index for the castor-oil-based foam. Interestingly, the castor-oil foam and the extrapolated 100% soy foam suggested nearly the same air flow values at an index of 102. The explanation for the difference in the dependence on index for the castor systems was believed to be principally due to an increase in the number of closed-cell windows (even after crushing) with increasing index for the castor-oil foam, as discussed in part I of this two-part report. As expected, however, we did find a systematic decrease in the tear and tensile values; this was also the case for both the 25% IFD and 65% IFD values, with a decrease in the index due to fact that a lower index led to a more poorly developed chemical network, but it also could often promote a higher elongation and higher compression set because the network was looser and slightly lower in $T_g$. Indeed, Figure 7(a–f) provides distinct support for these expectancies, although the 50% compression set did not show a major increase with decreasing index until the lower most value, that is, 84. What was not as easily predicted, however, was that the SF did show a decrease with increasing index; this implied that the two IFD values were not equally affected by the index, and this led to an alteration of the ratio of these two well known values that provide the value of SF [see Fig. 7(f)]. In addition to the index affecting IFD directly, it also did so indirectly by influencing the air flow, which in turn, also altered the true IFD of the foam product.

With regard to how the index influenced the force recovery kinetics after compression, Figures 8(a,b) provides this information. As expected, there was, in general, a more rapid growth to the force as the index increased because of the presence of a better chemical network caused by a closer stoichiometric balance of hydroxyl to isocyanate functionalities. The data were not completely systematic in this regard, although the trend was present, particularly for the U-1000 and soy-containing foams relative to the castor-oil foam. This not completely systematic behavior may also have been due to the fact that as the index increased, although there was a better network formed, there was also a systematic increase in $T_g$ and as some broadening of that dispersion [recall Fig. 1(b) of this report and also Figs. 8(b) and 14(b) from part I of this article], which in turn, tended to slow the recovery kinetics because a more glassy (more viscous) system will display

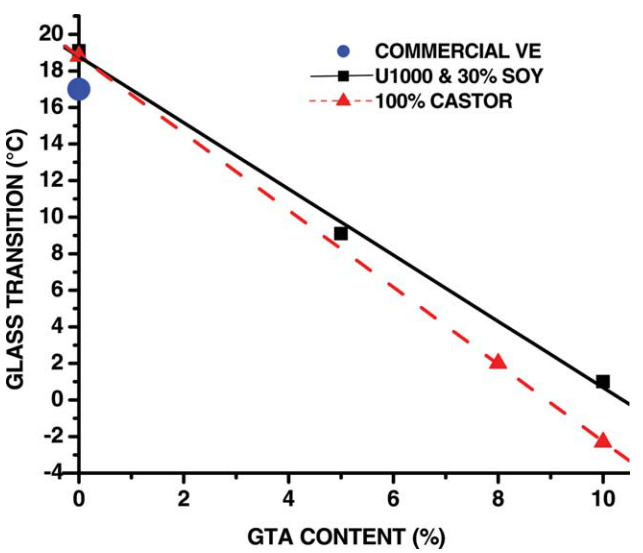


**Figure 9** $T_g$ of the U-1000–30% soy-oil, 100% castor-oil, and Tempur-Pedic VE foams as a function of the GTA content. [Color figure can be viewed in the online issue, which is available at wileyonlinelibrary.com.]

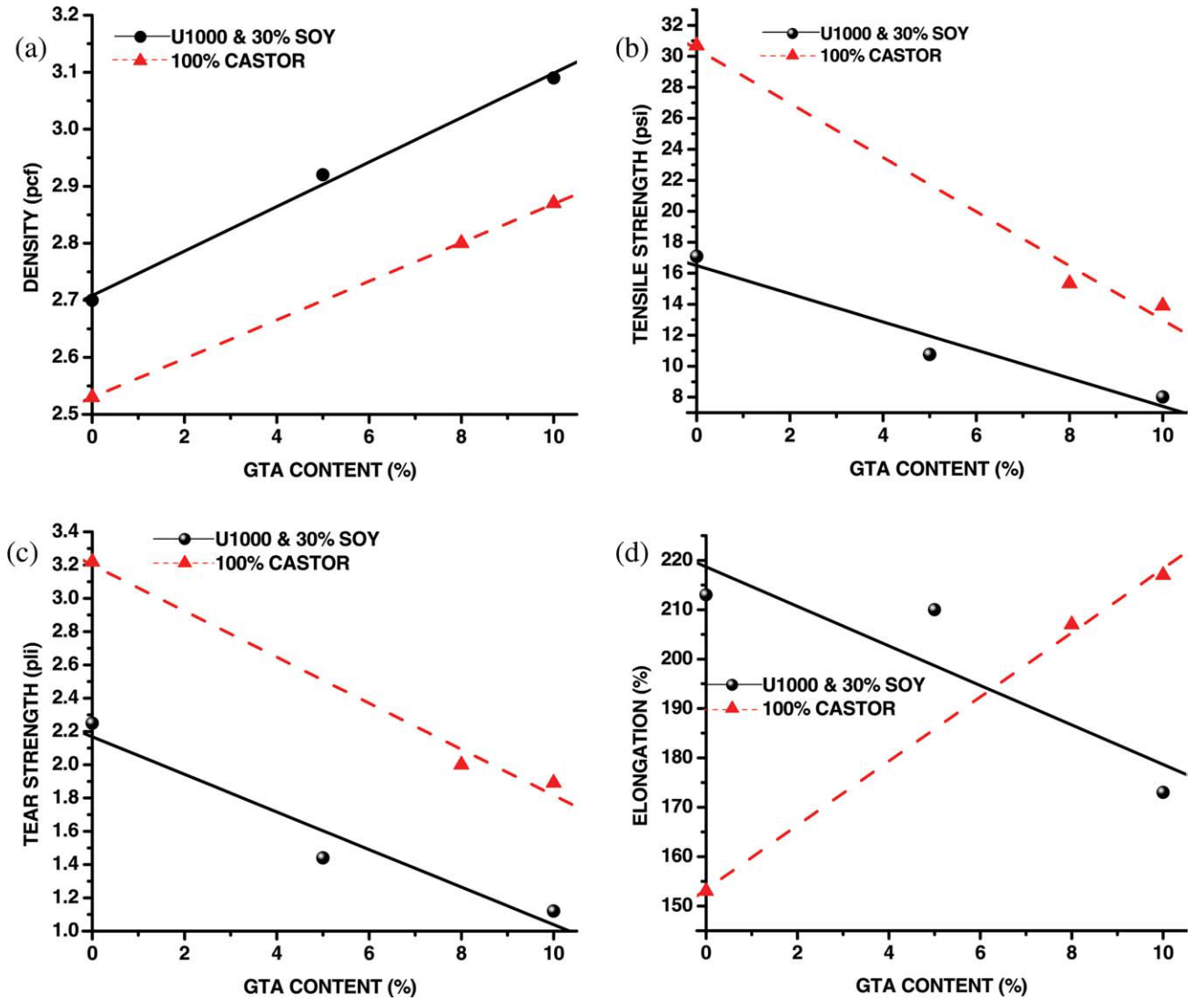


**Figure 10** (a) Density, (b) tensile strength, (c) tear strength, and (d) elongation of the U-1000–30% soy and 100% castor-oil foams as a function of the GTA content. [Color figure can be viewed in the online issue, which is available at wileyonlinelibrary.com.]

more sluggish kinetics, even if it possesses a better network structure. Likewise, when the hysteresis was calculated for the two types of vegetable-oil-based foams, we also found that the data for this parameter, although tending to decrease as expected with increasing index, showed scatter and are, therefore, not given here. However, the hysteresis values were in the general range of 50–75%, which was lower than those for the more dense commercial VE foam, which had a value of 93%; it was likely higher because of its greater density. As shown when we address the incorporation of the plasticizer below, this had an important effect on increasing the hysteresis, particularly for the castor-oil foam.

Turning to the effects of the one plasticizer studied (GTA), we focus first on the parameter of $T_g$. As shown in Figure 9, not surprisingly, a higher content of GTA lowered $T_g$ accordingly in a linear manner for the range covered; likely, this linear relationship would not be valid over a wider range for reasons that have been noted and discussed for many more highly plasticized polymeric materials.[12–14] One would also expect that for a given foam formulation that had added plasticizer, there would also be a somewhat enhanced density of the final foam because the plasticizer is added weight without any additional isocyanate and water to undergo the foaming reaction. Indeed, as shown in Figure 10(a), this was exactly what we observed, and a linear relationship was noted for each of the two systems. Although the density change was not major and, thus, did not influence the cell size significantly, it was very systematic in its effect. Furthermore, as expected, increasing plasticizer content distinctly

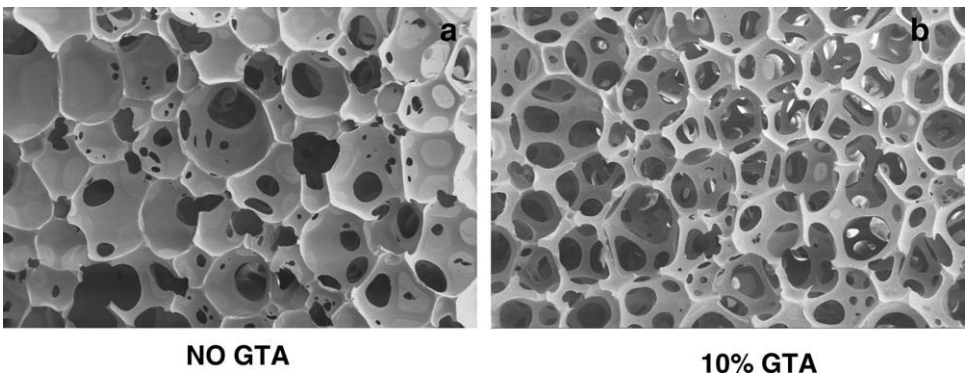


**Figure 11** SEM micrographs of the 100% castor-oil foams (a) without and (b) with GTA.

lowered the tensile and tear values, partially because of a decrease in $T_g$ [particularly when in the $T_g$ region; see Figs. 10(b,c)]. However, it was, at first, very surprising that the two different systems displayed very distinctly opposing behaviors for the parameter of elongation to break in tension [see Fig. 10(d)]. This major difference in behavior was distinctly believed to be due to the major change in cell morphology that GTA caused for the castor-oil foam. Specifically, although GTA did not significantly change the cell texture for the U-1000 or its soy-containing foams, it did have a pronounced effect on inducing a much more open-cell texture for the castor-oil material, although cell size was not significantly altered. Figure 11(a,b) shows the castor-oil foam with no GTA [Fig. 11(a)] and with 10% addition of GTA [Fig. 11(b)]. This great difference clearly showed that GTA served as an effective cell opener in this specific system, for we noted this very distinct textural change in morphology at the cellular level each time that GTA was incorporated into the castor-oil system. Therefore, this distinct change in the cell morphology also had, not surprisingly, a major effect on the air flow for the castor-oil system, as shown in Figure 12. However, little change in the air flow occurred for the U-1000–soy series because its cell structure for the U-1000–soy series was affected little by GTA.

The effect of the GTA content also had an influence on the IFD values (25 and 65%) but for only the castor-oil foam, as shown in Figure 13, which provides data for both the soy and castor-oil foams. In particular, the IFD values at either deflection percentage were hardly changed when GTA was added to the soy-containing foam, but it systematically decreased with GTA content for the castor-oil

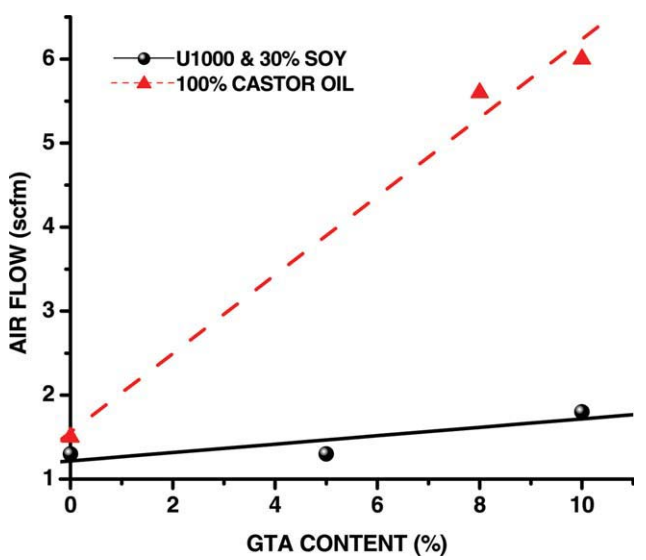


**Figure 12** Air flow of the U-1000–30% soy and 100% castor-oil foams as a function of the GTA content. [Color figure can be viewed in the online issue, which is available at wileyonlinelibrary.com.]

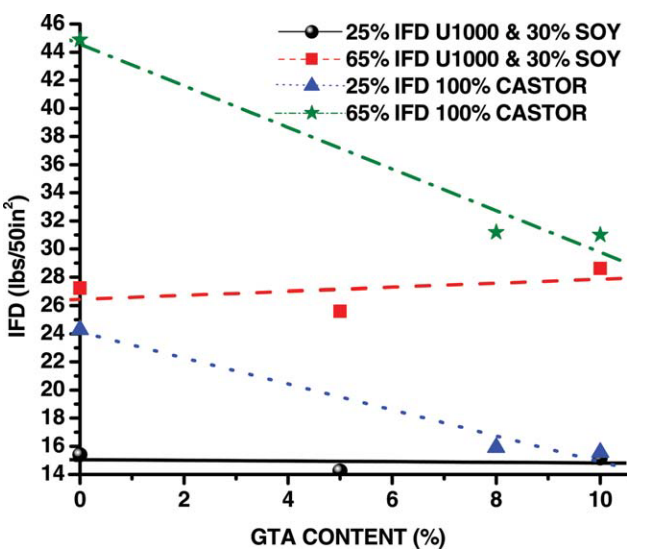


**Figure 13** 25% IFD and 65% IFD for the U-1000–30% soy and 100% castor-oil foams as a function of the GTA content. [Color figure can be viewed in the online issue, which is available at wileyonlinelibrary.com.]

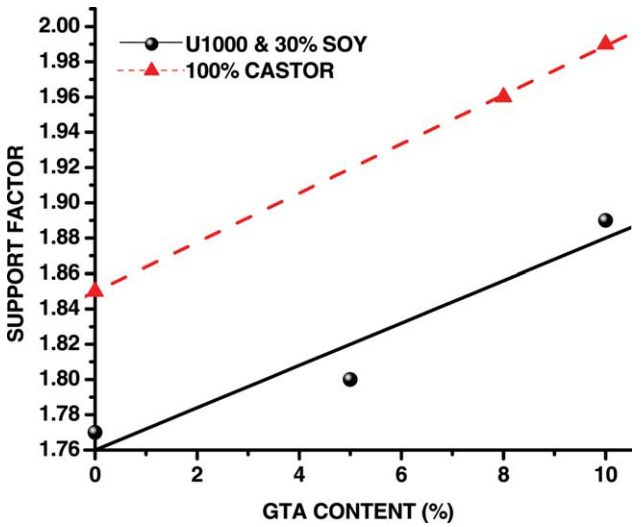


**Figure 14** SF for the U-1000–30% soy and 100% castor-oil foams as a function of the GTA content. [Color figure can be viewed in the online issue, which is available at wileyonlinelibrary.com.]

foam. Interestingly, when SF was determined for the two foam types (see Fig. 14), each still showed a linear increase with GTA content, but we also recognized that the magnitude of the change was relatively small. This latter point also applied to the relative difference between the U-1000 soy-containing foam and that of the castor-oil foam for a given GTA level. When the hysteresis was calculated for the vegetable-oil-based foams, the effect of GTA was to increase the hysteresis, as shown in Figure 15. In fact, this figure shows particularly that the effect of GTA on the hysteresis behavior was much stronger for the castor-oil foam than for those of the U-1000–soy series. Clearly, the data indicate that a possibly slightly higher amount of GTA might have provided a hysteresis value nearly equivalent to that of the commercial VE foam (see Table I). However, the level of 50% compression set for the two types of vegetable-oil foams as a function of GTA was significant, in that although the set did not change that much for either foam with GTA (see Fig. 16), the U-1000 soy-containing foams did indicate a distinctly higher set value; this, we believe, was due to the 100% higher sol fraction that occurred for the soy-containing foam versus that of the castor-oil foam [see Fig. 1(a)]. Also, even with the significant change in cell morphology with GTA addition, the compression set was not greatly influenced relative to its behavior without any GTA addition. This logically implies that cell morphology was not the critical factor here in influencing the set, but rather it was the network character, specifically the cross-linking character, of the solid portion of the foam that dominated this physical property.

With regard to the effect of GTA on the force recovery kinetics for the soy-containing foam and the castor-oil foam, the results are shown in Figure 17(a,b). It was clear from these data that GTA had a distinct enhancing effect on the recovery kinetics and the level of recovery force for the time window used for this test, particularly for the castor-oil foam. This major effect for either system is strongly believed to have been principally due to the

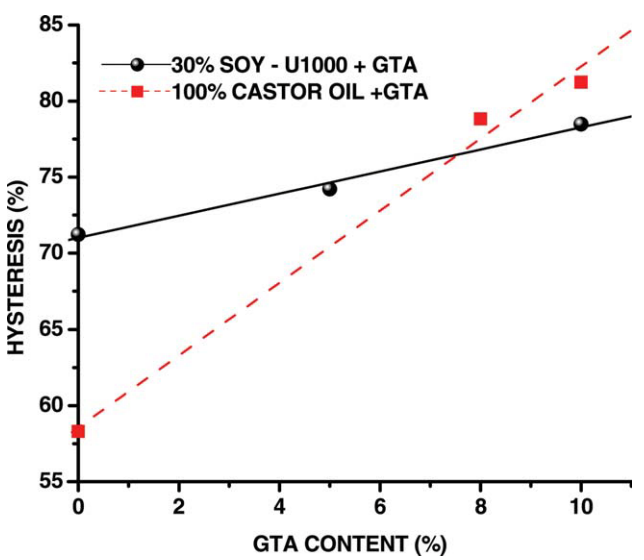


**Figure 15** Hysteresis for the U-1000–30% soy and 100% castor-oil foams as a function of the GTA content. [Color figure can be viewed in the online issue, which is available at wileyonlinelibrary.com.]

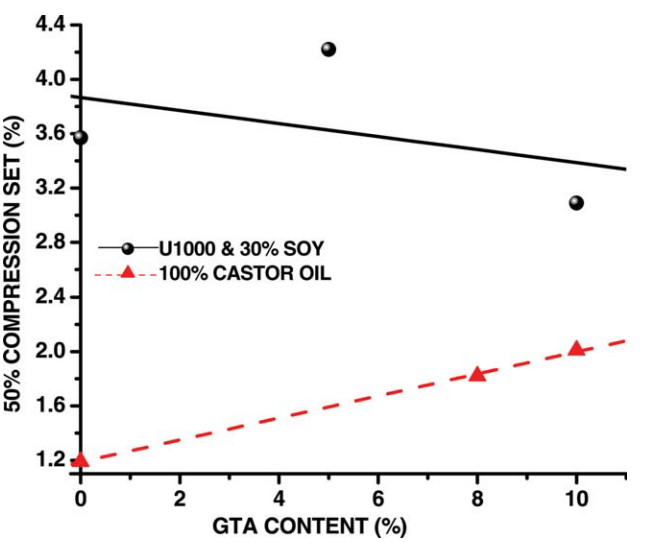


**Figure 16** 50% compression set for the U-1000–30% soy and 100% castor-oil foams as a function of the GTA content. [Color figure can be viewed in the online issue, which is available at wileyonlinelibrary.com.]

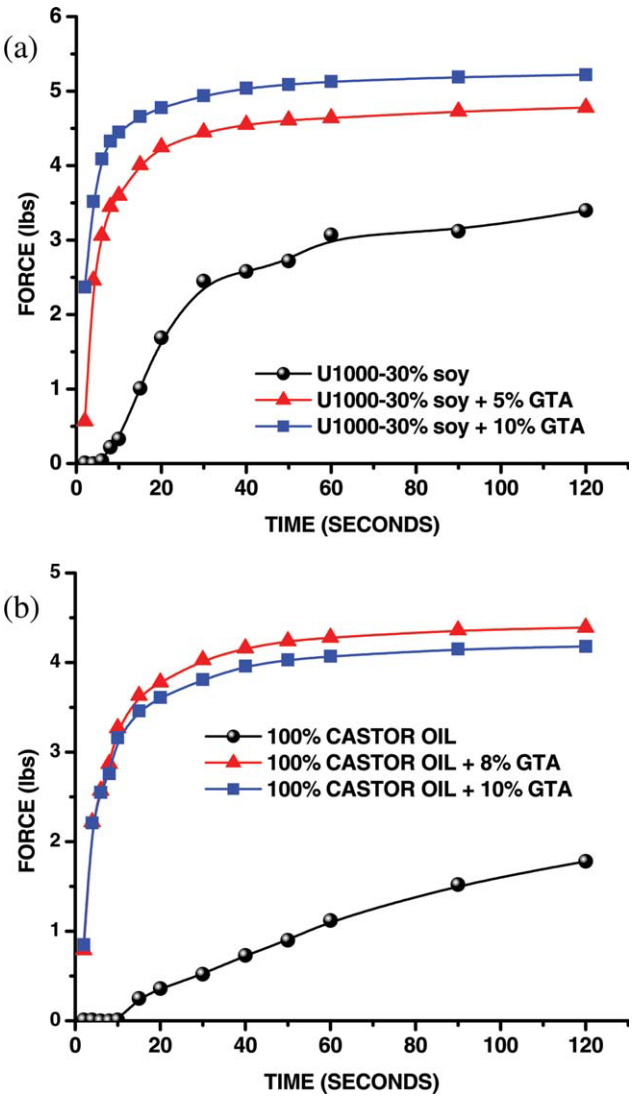


**Figure 17** Force recovery for the (a) U-1000–30% soy foams and (b) 100% castor-oil foams as a function of the GTA content. [Color figure can be viewed in the online issue, which is available at wileyonlinelibrary.com.]

depression in $T_g$ with GTA addition that although it lowered the modulus of the material, allowed a much more rapid elastic, less glassy (less viscous) response on recovery. However, the effect of a more open cell structure caused by the GTA component should also aid the recovery kinetics.

### Ball rebound (resilience) and comparison with earlier DMA damping behavior

One of the particularly important areas that our two-part report addresses is that of the damping behavior of the foams. In part I, we provided damping data obtained via DMA measurement of tan δ in the linear VE region at a frequency of 1 Hz, and we also briefly addressed how the damping peak shifted with frequency, at least for selected samples. In the Introductions of parts I and II, we pointed out that resilience, which is sort of an inverse damping, is commonly determined by the use of a simple ASTM test known as ball rebound (rebound).[1] In particular, a specified thickness of foam is brought to a given temperature (and humidity if desired), and a steel ball 16 mm in diameter is dropped from a given height, and the level of rebound (height) is a measure of resilience, as expressed in percentage of the drop distance. That is, a small rebound implies a low resilience (high damping), whereas a high rebound implies a high resilience (elastic rubberlike behavior). For example, 100% rebound would signify fully elastic behavior, whereas 0% rebound would indicate fully viscous behavior and, thus, the highest level of damping.

We also questioned in the early part of this report whether there should necessarily be a one-to-one correlation between the damping behavior determined by this method relative to that obtained by the DMA method because the latter is a constant frequency (rate) method applied in the linear VE region and the rebound method is not a constant rate deformation in that the ball slows to zero speed from its initial velocity on impact. Another difference between the ball-rebound test and that of DMA damping is that the ball-rebound test is a first cycle test in which the sample has not undergone any previous loading in the test area before the actual test, whereas in a DMA test, the sample has already experienced many cycles of very small strain before the damping is recorded at a given temperature. Furthermore, depending on the material measured during the rebound test, the deformation may not necessarily reside in the linear region, particularly for cellular materials where the deformation near the surface of impact may be greater than that somewhat below the surface because it is the surface region where the ball impact is first felt. In fact, one could anticipate that the mass of the ball would likely be influential in this regard, but we do not address this parameter here but rather use the ball mass/size that is specified by the ASTM 3574-H protocol. Finally, one would expect, at least in the case of foams with low air flow due to low cell opening, that the ball impact in the rebound test may not allow for rapid air flow from the cells; this might, thereby, affect the rebound value. This latter point is more applicable to so-called tight foams, where the air flow is extremely limited because of a high population of closed cells. Hence, on the basis of the issues that have been raised, we attempt to shed some light on the level of damping determined by these two methods of DMA and ball rebound for the VE foams discussed in this article. Specifically, to make such a comparison, we obtained rebound data on foams that were equilibrated to a specific

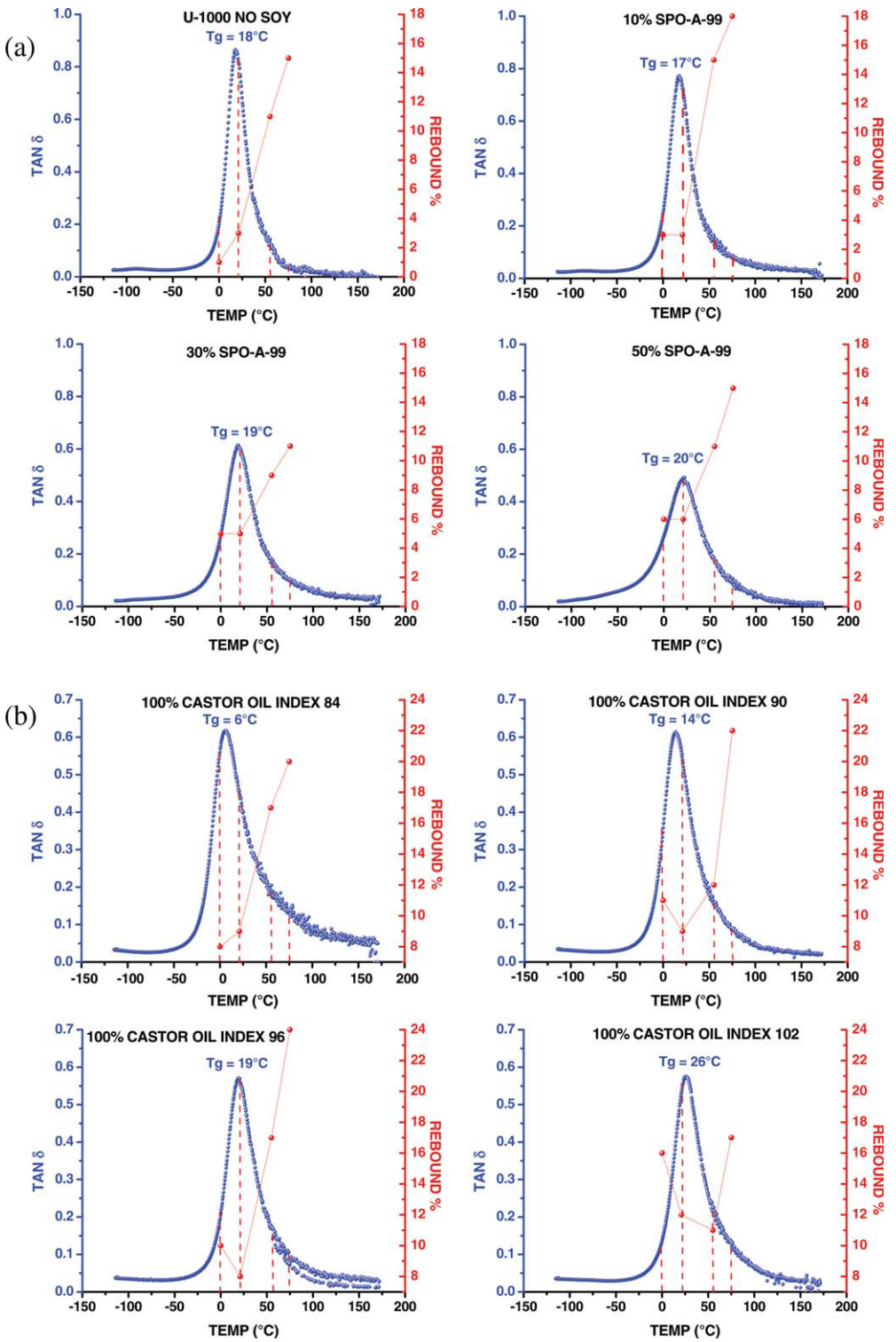


**Figure 18** Ball rebound as a function of the temperature versus tan δ for the VE foams with different (a) soy and (b) castor-oil contents (1 Hz). SPO-A-99 = Biobased Technologies polyol Agrol 3.0 with a hydroxyl number of 99 or BBT-99. [Color figure can be viewed in the online issue, which is available at wileyonlinelibrary.com.]

temperature. We then plotted the corresponding tan δ behavior and the rebound data together for a given foam as a function of temperature. Two examples of this are provided in Figures 18(a,b). Figure 18(a) provides the data for the soy content series at a constant index of 96, but the soy polyol content was systematically varied from 0 to 50%, which led to a slight increase in $T_g$ and some loss in the tan δ peak magnitude along with some increase in the $T_g$ dispersion breath. The data given

in Figure 18(b) is for the index study of the castor-oil foams. Both of these series provided some interesting observations. Each showed, in general, that there was quite a good correlation between the two methods from the range of temperature covering the peak value of tan δ and upward to higher temperatures as the material became more elastic and rubberlike. This lent credence to the choice of the frequency of 1 Hz used for the DMA measurement because the peak tan δ value appeared to be located at nearly the same temperature, where the rebound was at a minimum. In other words, we noted, in general, that for every one of the eight foams, the rebound increased as tan δ decreased from its peak value. However, on the lower temperature side of the peak tan δ value, this was not always the case; we observed, with an exception or two, that the rebound was lower or about equal to the value it showed near the peak tan δ for the given sample. This was certainly true for all of the U-1000–soy foam series and one of the castor-oil foams, whereas the remaining three of the latter series showed that the rebound did increase somewhat on the lower temperature side of the peak. However, even in the case of the latter three samples, some showed that even for comparable tan δ values on either side of the peak value, the rebound was distinctly less for the low-temperature side. What we believe that all of these data from the eight samples indicated is that rebound and DMA tan δ damping were quite well correlated, as stated before, for the high-temperature region of the tan δ dispersion but less clearly correlated on the lower temperature side.

One possible explanation for the behavior addressed previously is that on the lower temperature side where the material properties rapidly gained in stiffness, the ball deformation may have been more localized near the surface of the foam relative to when the ball struck a more rubberlike cellular material, as would have been the behavior on the upper temperature side. This may have led to nonlinearity in the deformation behavior with the rebound method; however, in DMA, the deformation was maintained in the linear region throughout the entire range of temperatures covered in the test. Thus, although the tan δ dispersion suggests that the damping is essentially a double-valued function except at its peak, one may not necessarily expect the rebound method to provide equal damping behavior at these same two temperatures where tan δ is equal. Further effort on a more complete study just of this topic is likely an area worthy of further investigation for future studies. Although in the previous discussion we focused on the comparison/correlation of rebound with tan δ, we also want to point out that the actual single values of rebound typically reported in accordance with the ASTM procedure

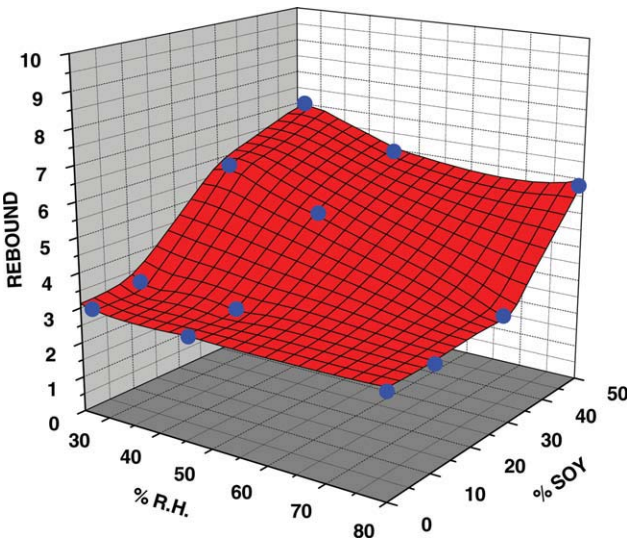


**Figure 19** Rebound as a function of the percentage RH and percentage soy at 21°C. [Color figure can be viewed in the online issue, which is available at wileyonlinelibrary.com.]

were lowest for the commercial VE foams (1%) relative to the vegetable-based forms of either type, whose values were no lower than 8%. Although the rebound values of high resilience foams were above 50%, acceptable values for VE foams were below 15%, so this implied that some of our prepared foams were a bit above this value, but this was not surprising because we did not specifically focus on placing the tan δ peak at a temperature exactly equivalent to that of the commercial VE material but rather systematically varied specific parameters, such as index and plasticizer content, to shift the tan δ peak, which in some cases, also affected the magnitude and breadth of the $T_g$ dispersion. Also, as indicated previously, a direct comparison of the rebound values of our foams with that of the value from the commercial VE foam was not particularly a truly fair comparison because that latter foam was, as stated earlier in this report, nearly twice as dense relative to those incorporating vegetable-based polyols. Rather, the message we wish to promote is that although our foams may not be fully optimized for maximizing the damping under ASTM conditions, we demonstrated how this property and several others are very much in line with the properties expected from acceptable VE PUFs.

### Effect of RH on the rebound

As indicated in the Introduction, we also carried out some limited studies of the influence of RH on the resilience or rebound properties of a 100% castor-oil foam and also some of the soy-containing foams. Figure 19 shows the response surface of rebound when plotted against both RH and soy content up to 50%

with a constant hydroxyl of 99. We observed that at a given soy content, there was not a strong influence of RH (as measured at 21°C) across the range of soy polyol contents. This lack of any strong dependence of rebound on RH was also true for the 100% castor-oil foam, which was equilibrated as well to different RH values (data not shown). However, as shown in Figure 19, at a constant RH, the dependence of rebound did become more significant on soy content in that rebound increased with the percentage soy, particularly above levels of 10%, and the strength of this dependence was greater at lower RH levels.

## CONCLUSIONS

In this report and in part I of this two-part series, we have shown that acceptable VE PUFs can be prepared with by either the substitution of a portion of soy-based polyols for those of petroleum origin or possibly even a fully vegetable-based polyol. Although the VE foams discussed in these two reports were not necessarily optimized, we have shown how their behavior can be manipulated in terms of modifying the $T_g$ dispersion, modulus, and so on by different approaches fundamental to polymeric materials in general, for example, the addition of plasticizer or changing isocyanate index. We, therefore, believe that such methodology can be used with further effort to produce suitable VE foams with less dependence on the need for petroleum-based polyols.

The authors thank Stanley Hager and Richard Skorpenske of Bayer MaterialScience for the donated Bayer polyols and the use of Bayer analytical facilities and for the many helpful discussions and value input associated with this study.

## References

1. Herrington, R.; Hock, K. Dow Polyurethanes: Flexible Foams; Dow Chemical; University Microfilms International, Ann Arbor, MI, 1997.
2. Armistead, J. P. In Chemical Engineering; Virginia Tech: Blacksburg, VA, 1985; p 236.
3. Woods, G. The ICI Polyurethanes Book; Wiley: New York, 1987.
4. Neff, R.; Dakin, S.; Green, T.; Gummaraju, R.; Smiecinski, T. Presented at Polyurethanes Conference, Las Vegas, NV, Oct 2004.
5. Hager, S.; Skorpenske, R. Proceedings of the Polyurethane Foam Association Technical Program, Arlington, VA, May 2001; 2001; Vol. 10.
6. Smiecinski, T. M.; Neff, R. A. Proceedings of the API Polyurethanes Technical Conference, Salt Lake City, UT, 2006; 2006; p 405.
7. Tobushi, H.; Okumura, K.; Endo, M.; Hayashi, S. J Intel Syst Str 2001, 12, 283.
8. Farkas, P.; Stanciu, R.; Mendoza, L. J Cell Plast 2002, 38, 341.
9. Delk, V.; Polk, R.; Prange, R.; Aguirre, F. Proceedings of the Annual SPI Polyurethanes Technical/Marketing Conference, Las Vegas, NV, 2004; 2004; p 35.
10. Das, S.; Mahendra, D.; Wilkes, G. L. J Appl Polym Sci 2008, 112, 299.
11. Alfredo, L.; Barb, D.; Shrock, A.; Bhatacharjee, D. Presented at Polyurethanes 2007 Technical Conference in Partnership with UTECH North America, Orlando, FL, 2008.
12. Ferry, J. Viscoelastic Properties of Polymers; Wiley: New York, 1981.
13. Van Krevelen, D. W. Properties of Polymers: Their Correlation with Chemical Structure, Their Numerical Estimation and Prediction from Additive Group Contributions; Elsevier: New York, 1990.
14. Sperling, L. H.; Fay, J. J. Polym Adv Technol 1991, 2, 49.